crystals

MDPI

Article

Effect of Hydrated Deep Eutectic Solvents on the Thermal Stability of DNA

Mariagrazia Tortora [1,2,*], Jacopo Vigna [3], Ines Mancini [3], Andrea Mele [4], Alessandro Gessini [2], Claudio Masciovecchio [2] and Barbara Rossi [2,3]

1 AREA SCIENCE PARK, Padriciano, 99, 34149 Trieste, Italy
2 Elettra-Sincrotrone Trieste, S.S. 114 km 163.5, Basovizza, 34149 Trieste, Italy; alessandro.gessini@elettra.eu (A.G.); claudio.masciovecchio@elettra.eu (C.M.); barbara.rossi@elettra.eu (B.R.)
3 Laboratory of Bioorganic Chemistry, Department of Physics, University of Trento, Via Sommarive, 14, 8123 Trento, Italy; jacopo.vigna@unitn.it (J.V.); ines.mancini@unitn.it (I.M.)
4 Department of Chemistry, Materials and Chemical Engineering "G. Natta", Politecnico di Milano, Piazza L. da Vinci 32, 20133 Milano, Italy; andrea.mele@polimi.it
* Correspondence: mariagrazia.tortora@elettra.eu

Abstract: DNA's structure stability in hydrated deep eutectic solvents (DESs) is getting growing attention for emerging bio-applications. The employment of DESs as novel co-solvents in water media could favor eco-friendly and biodegradable materials for DNA storage and handling. Understanding the molecular interactions between nucleic acids and aqueous DES is crucial for developing new-generation solvents for biomolecules. In this work, we exploit the molecular sensitivity and selectivity of synchrotron radiation UV resonance raman (SR-UVRR) spectroscopy to explore the interplay between a choline chloride:urea (ChCl:U) DES and double-stranded DNA. Our study analyzes the impact of ChCl:U on the DNA's thermal unfolding pathway by focusing on the guanine nucleobases whose Raman signal could be strongly enhanced through careful tuning of the excitation wavelength.

Keywords: DNA; deep eutectic solvents; UV resonance raman; structural transitions

Citation: Tortora, M.; Vigna, J.; Mancini, I.; Mele, A.; Gessini, A.; Masciovecchio, C.; Rossi, B. Effect of Hydrated Deep Eutectic Solvents on the Thermal Stability of DNA. *Crystals* **2021**, *11*, 1057. https://doi.org/10.3390/cryst11091057

Academic Editors: Lorenzo Gontrani and Matteo Bonomo

Received: 16 July 2021
Accepted: 30 August 2021
Published: 2 September 2021

1. Introduction

A common feature of recent research in green chemistry is the investigation of new eco-sustainable solvents. Deep eutectic solvents (DESs) have recently been proposed as an environmentally friendly alternative to organic solvents and ionic liquids (ILs) [1–3]. Compared to ILs in particular, DESs are cheap, easy to prepare from many and widely available starting materials, non-toxic, and biodegradable. Among the DESs, natural deep eutectic solvents (NaDESs) are getting growing attention for their improved biocompatibility, being prepared from natural compounds such as amino acids, sugars, and choline. Because of their tailorable physicochemical properties, NaDESs are increasingly used in many processes, such as pharmaceuticals, therapeutics, biotransformation, nucleic acid manipulation, and biocatalysis [4–7]. DNA solutions may experience denaturation because of oxidative and hydrolytic phenomena. In addition, the variation of medium conditions (temperature, pH, and ionic strength) can damage the DNA helix structure [8,9]. From this point of view, the search for new solvents that ensure a greater stability and more efficient extraction and handling processes is becoming increasingly relevant. The stability and solubility of duplex DNA in DES have been examined by several previous studies [10–15]. They have shown that the use of DESs as solvents, anhydrous or in water, guarantees the stability of DNA duplexes for long periods and at high temperatures [12,16]. Many researchers suggest DESs can establish multi levels and specific interactions, such as electrostatic attraction, hydrophobic and polar interactions with DNA major and minor grooves, and multiple hydrogen bonding [12,14,15]. Depending on the systems investigated, the DESs' cations binding on DNA major or minor grooves and specific interplays with DNA bases have been proposed.

This work aims to explore the effectiveness of the choline chloride:urea (ChCl:U) DES as co-solvent of water in improving the thermal–structural stability of double-stranded DNA. The mixture choline chloride:urea 1:2, sometimes referred to as reline [17], is the most popular DES of type III (i.e., a mixture of a quaternary ammonium salt with a molecular H-bond donor, according to the DES classification summarized in Table 1 of the paper by Smith, Abbot, and Ryder [3]). Such a popularity made reline a kind of benchmark for DESs, especially given the thorough physico-chemical characterization present in the literature. These facts thus prompted us to use reline as a natural "first choice" for this brand-new investigation on DES–DNA interaction. As recently reported [18–21], the synchrotron radiation UV resonance raman (SR-UVRR) spectroscopy gives promising results in the selective probing of the local order–disorder or conformational transitions in large nucleic acid molecules. We have shown the technique to provide the molecular sensitivity needed to monitor subtle changes in base geometry and local intra- and intermolecular interactions of DNA dissolved in aqueous solutions of ionic liquids [18,19,21]. These studies revealed the important role played by guanine bases in the DNA groove that are preferentially involved in interactions with the imidazolium cations of ILs [19,21]. Such strong cation-mediated forces seem to be responsible for a more effective stacking between guanine residues, even at higher temperature values, which is consistent with the improved thermal stability of the double-helix structure of DNA [21]. Interestingly, the stabilization effect operated by imidazolium-based ILs on large molecules of DNA is found to be further enhanced as the alkyl chain on the imidazolium cation gets shorter [21]. By exploiting the same experimental approach, UVRR experiments have been implemented here to provide insights into the base stacking, hydrogen-bond breaking, and backbone conformation of DNA dissolved in aqueous solutions of a DES. The choice of the excitation wavelength allows to selectively focus, during the thermal unfolding pathway of DNA, on the interactions between the DES molecules and specific guanine and thymine tracts in the sequence of nucleic acids. The comparison of Raman results with those obtained from Circular Dichroism (CD) absorbance measurements leads to a comprehensive characterization of the structural motifs and of the intermolecular interactions of DNA in hydrated DES, possibly affecting the thermal stability of the DNA structure.

2. Materials and Methods

UVRR spectra were collected by means of the synchrotron-based UVRR setup available at the BL10.2-IUVS beamline of Elettra Sincrotrone Trieste (Italy) [20]. The exciting wavelength was set at 250 nm by regulating the undulator gap and using a Czerny-Turner monochromator (Acton SP2750, Princeton Instruments, Acton, MA, USA) equipped with an 1800 groves/mm holographic grating for monochromatizing the incoming synchrotron radiation. Raman spectra were recorded in back-scattered geometry using a single pass of a Czerny-Turner spectrometer (Trivista 557, Princeton Instruments, MA, USA, 750 mm of focal length) and a holographic grating at 1800 g/mm. The spectral resolution was set at 1.9 cm^{-1}/pixel. The calibration of the spectrometer was standardized using cyclohexane (spectroscopic grade, Sigma-Aldrich Chemie GmbH, Schnelldorf, Germany). The final radiation power measured on the samples was about 40 µW. Any possible photo-damage effect due to prolonged exposure of the sample to UV radiation was avoided by continuously spinning the sample cell during the measurements.

Circular Dichroism analyses were performed at room temperature using a Jasco J-710 polarimeter (Jasco Europe S.R.L., Cremella (LC) Italy). Each CD spectrum was averaged over 10 scans recorded in the range from 220 to 400 nm, at a scanning speed of 500 nm/min and 1 nm of bandwidth. Measurements were performed under a constant nitrogen flow, to purge the ozone generated by the light source of the instrument.

DNA sodium salt from salmon testes (sDNA) (CAS number 438545-06-3, ~2000 base-pairs, MW = 1.3×10^6 Da, % G-C content: 41.2%), choline chloride (ChCl), and urea (U) were purchased from Sigma-Aldrich and used without further purification. Before use, ChCl and U have been dried under vacuum with phosphorus pentoxide for 48 h to remove

any water contamination. For UVRR experiments, sDNA solutions at a concentration of 0.2 mM (0.25 mg/mL) were obtained by dissolving lyophilized powder of DNA in Tris buffer (10 mM at pH 7.4) and gently stirring for 24 h to achieve a limpid solution. The ChCl:U DES was prepared by mixing ChCl and U at a molar ratio of 1:2 and heating at 80 °C under stirring for some minutes to obtain a limpid viscous liquid. The preparation of the hydrated DES was done by simply mixing the pure DES with a known amount of Tris and then allowing the system to reach equilibrium. For the sDNA/ChCl:U samples, the hydrated DES was mixed with sDNA in a Tris solution to reach the final molar ratios of 158 and 474 DES molecules for each DNA base pair. All the solutions were freshly prepared for UVRR measurements and they appeared limpid before the running of experiments and after the thermal heating. For CD experiments, the sDNA and sDNA/ChCl:U samples were diluted 12 and 10 times in Tris with respect to the samples prepared for UVRR measurements.

3. Results

Figure 1a displays the UVRR spectra recorded at 300 K of sDNA in an aqueous buffer solution and sDNA dissolved in ChCl:U/Tris at two different molar concentrations, i.e., 158 and 474 DES molecules for each base pair. We have focused on the wavenumber region 1250–1850 cm^{-1}, where the main Raman signals associated with DNA nucleobases are found. As a first remark, it has to be noted that the spectra of sDNA in hydrated ChCl:U mainly resemble the vibrational profile of DNA in water, without any significant interfering signal arising from the DES (trace at the top in Figure 1a). This reliably allows us to analyze in detail the spectral modifications of the Raman bands associated with sDNA in the presence of DES.

The UVRR spectra reported in Figure 1 were collected using a 250 nm excitation wavelength. This choice is justified by the overlap of this excitation energy with the electronic transition localized on the double bond N7 = C8 of the imidazole ring of the purine bases, which satisfies the resonance condition for guanine dG and adenine dA residues [20–24]. The comparison between the UVRR profile of sDNA (Figure 1a) and the spectra of the deoxynucleotides 2′-deoxyadenosine 5′-triphosphate sodium salt solution (dA), 2′-deoxycytidine 5′-triphosphate disodium salt (dC), 2′-Deoxyguanosine 5′-triphosphate trisodium salt solution (dG), and thymidine 5′-triphosphate sodium salt solution (dT) reported in Figure 1b helps to identify the contribution of each nitrogenous base in the vibrational profile of the sDNA. The prominent signal dGI~1485 cm^{-1} in the spectrum of the sDNA is mainly attributed to the combination of the N7 = C8 and C8-N9 ring stretching and C8-H in-plane deformation of the dG purine group [22,25–27] as well as to the C6 = O stretching [28]. The contribution to the band at ~1485 cm^{-1} from the Raman signal of adenine can be considered negligible at the excitation wavelength of 250 nm due to the proximity of the 255 nm electronic transition of guanine [18,19,25]. The intensity and the frequency position of the dGI band in DNA are very sensitive markers of the base-stacking interactions and hydrogen bonds (H-bonds) involving the guanine residues [29–31]. The Raman signals from purine residues also include the broad band at ~1336 cm^{-1} in the spectrum of sDNA (labeled as dA + dG in Figure 1a) that results from the overlap between the base ring vibrations assigned to adenine dA and guanine dG residues [26,27]. This Raman signal is also diagnostic of the nucleoside conformations in DNA, thanks to the predominant imidazole ring character of the associated vibrational modes [22,26]. Finally, the large bump center at ~1637 cm^{-1} in the spectrum of sDNA (band labeled as dT in Figure 1a) is mainly related to the coupled stretching vibrations of C4 = O and C5 = C6 bonds of the dT residue [31,32]. Despite the relative complexity of this vibration, the large localization of the mode on the C4 = O group makes the signal dT~1637 cm^{-1} sensitive to any perturbation occurring at that site of the thymine base [33]. Figure 1a points out some alteration in the UVRR spectra of sDNA in the presence of ChCl:U. Hence, the downshifts of ~5 cm^{-1} of dGI, ~6 cm^{-1} of dA + dG, and ~10 cm^{-1} of dT bands exhibited by sDNA in the aqueous ChCl:U 1:158 sample reflect changes in

the hydrogen-bonding state on the proton-acceptor sites, mainly of guanine, adenine, and thymine residues [28,34]. The effects of choline-based DES on the thermal behavior of sDNA are reported in Figure 2. The graph shows the UVRR difference spectra for the sample of sDNA/ChCl:U, obtained by subtracting the spectrum at the lowest temperature, 300 K, from the Raman profiles measured at the indicated temperatures (intermediate traces in Figure 2). UVRR spectra of sDNA in hydrated ChCl:U at 300 and 375 K are also displayed at the bottom and at the top of Figure 2, respectively.

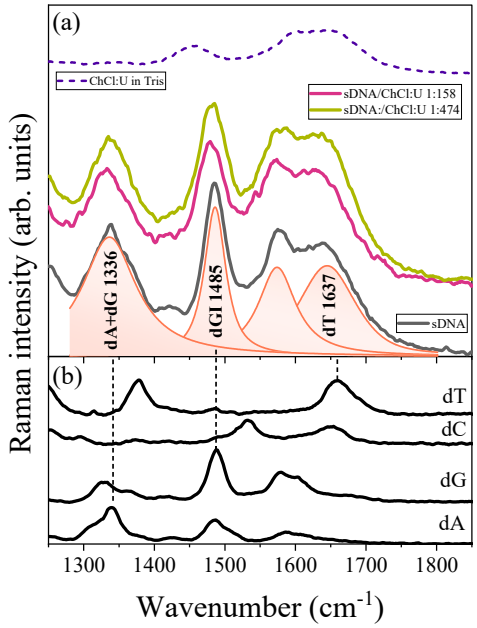

Figure 1. (**a**) 250 nm-excited Raman spectra of sDNA and sDNA/ChCl:U (1:158 and 1:474, respectively) collected at 300 K; the profile of the hydrated ChCl:U is reported for comparison in the same graph. (**b**) UVRR spectra of deoxynucleotides dA, dG, dC, and dT in a Tris buffer recorded using 250 nm as the excitation wavelength.

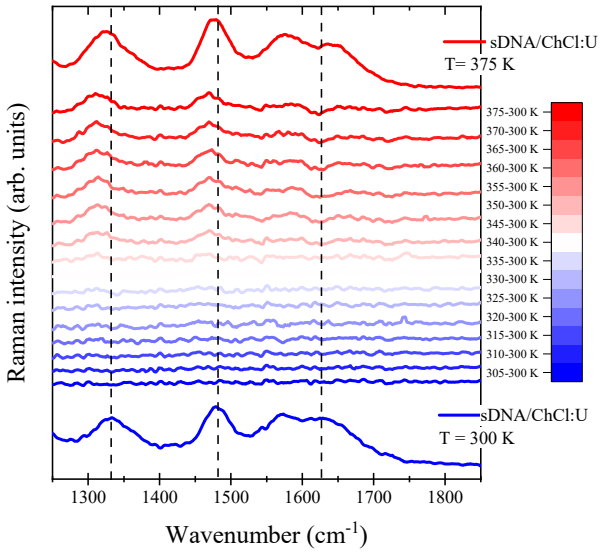

Figure 2. 250 nm-excited Raman spectra of sDNA/ChCl:U (1:158) collected at 300 K (bottom trace) and 375 K (top trace). Intermediate traces show the difference spectra computed by subtracting the spectrum measured at the lowest temperature, 300 K, from the spectrum at the indicated higher temperatures.

The different spectra in Figure 2 show that the Raman features of the sDNA at ~1336, 1485, and 1637 cm^{-1} are sensitive to temperature throughout the range 300–375 K, with the most pronounced spectral changes above 350 K. These heat-induced intensity and frequency modifications of the Raman bands of sDNA indicate that such vibrations can be adopted as markers of structural perturbations in sDNA, such as H-bond breaking, base unstacking, and the bases' conformational changes occurring in the double-stranded structure of DNA following an increment in temperature [8,18,19,30,33].

4. Discussion

As mentioned above, since the Raman band dGI of sDNA is mainly attributable to normal in-plane modes of the purine ring of guanine, the intensity of this signal is very sensitive to base-stacking interactions involving the guanine residues [18,24,27–30,34,35]. Figure 3a–c display the temperature-dependent intensity of the dGI Raman band of sDNA measured in an aqueous buffer solution and in hydrated ChCl:U. In each plot, the intensities have been normalized to their minimum and maximum values for a better comparison.

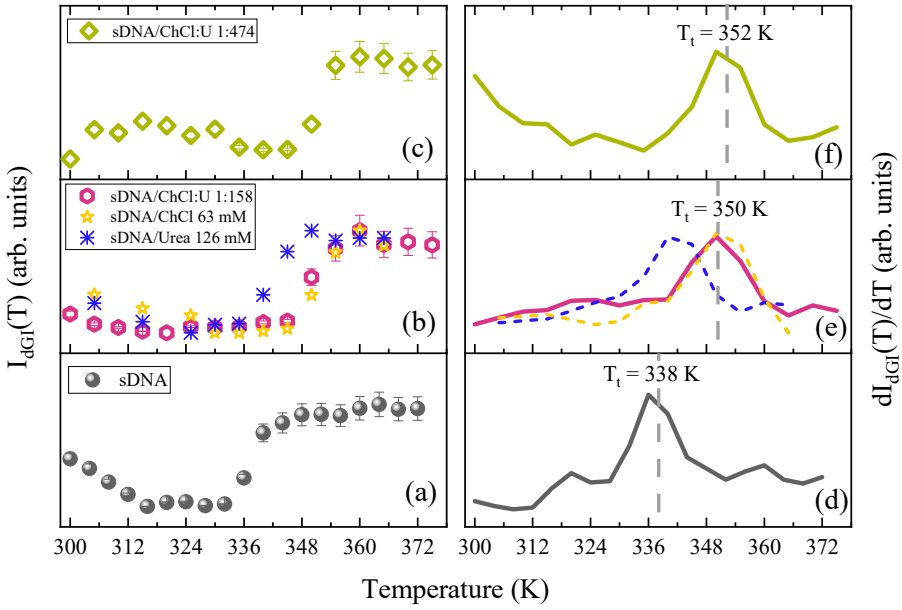

Figure 3. (**a**–**c**) Temperature dependence of the Raman intensity of the dGI band for sDNA and sDNA/ChCl:U (1:158 and 1:474); panel (**b**) shows also the temperature profiles of the dGI band obtained for sDNA in hydrated ChCl (63 mM in Tris) and in hydrated urea (126 mM in Tris). (**d**–**f**) First-derivative curves of the temperature profiles (**a**–**c**); the transition temperatures T_t obtained for sDNA without and with DES are marked in the corresponding panels.

The sigmoidal profile reported in Figure 3a shows a sudden increase in the dGI band's intensity (Raman hyperchromicity) for sDNA at about 340 K, suggesting the occurrence of a cooperative structural transformation of the double-helix sDNA structure. The intensity recovery of the dGI band relates to two possible effects: (i) H-bond breaking and base unstacking; and (ii) local structural changes, such as enhanced base mobility and base tilting specifically involving guanine residues in the structure of DNA [18,25,27,30,33,35]. The first-order derivative of the dGI band temperature profile (Figure 3d) exhibits almost a mono-phasic behavior, pointing out the occurrence of a unique cooperative structural transition in the explored temperature range for sDNA. The derivative maximum of the curve in Figure 3d provides a quantitative estimation of the transition temperature $T_t \simeq 338$ K between the initial and the final thermal stage for sDNA. Interestingly, comparing the traces in Figure 3, the effect exerted by the ChCl:U DES on the local structural modifications of the G-tracts during the thermal pathway of sDNA comes out. The first-derivative curves in Figure 3e,f, in fact, indicate a significant increment in T_t from 338 K for sDNA

in Tris up to 350 and 352 K for sDNA dissolved in aqueous ChCl:U at a concentration of 158 and 474 of DES molecules for each sDNA base pair, respectively. This issue seems to contradict previous studies [14,36] about the relative stability of DNA sequences in anhydrous and hydrated DESs. In these works, the authors attributed the observed change in the secondary structure and the reduction of the melting temperatures of sDNA to the dehydration effect caused by ChCl:U DES. Differently from the average melting process probed by UV absorption of sDNA discussed in the mentioned investigations, the UVRR guanine transition temperature should be interpreted as a process involving local events and cooperative conformational changes specifically affecting DNA dGI base tracts. In this view, the establishment of strong H-bonds between the DESs' components and dG tracts and the consequent partial dehydration of sDNA can be described as the key factors that cause the increasing in T_t and that stabilize sDNA in hydrated ChCl:U. In Figure 3b, we have included the dGI band intensity curves acquired for the urea and sDNA/ChCl solutions in the same relative concentrations of sample sDNA/ChCl:U 1:158, to gain further insight into the role played by the individual DES components in interacting with sDNA. The ChCl moiety seems to be involved in stronger interplays with guanine residues compared to urea and to be the first responsible for the increment in T_t, as also evidenced by its first-derivative in Figure 3e. It has been reported the ability of choline ions to stabilize sDNA [12] and the predominant activity of cations in reducing the repulsive forces between the phosphate groups of the DNA strands. In particular, Nakano et al. [15] have shown that choline ions linger around DNA even though the strength of the hydrogen bond is weak and stabilize a DNA duplex more effectively than sodium ions. In the same graphs, we can notice how urea slightly influences the dGI traces thermal pathway and that its profiles almost resemble those of sDNA in Tris. When urea is in solution with DNA, it is randomly distributed between the DNA's domain and it tends to replace water molecules in the first hydration shell around the DNA at increasing concentrations, thanks to its great hydrogen-bonding capacity [11,37]. Nonetheless, only when DNA double strands are in the unfolding state urea reveals its preferential interactions with the polar amide surfaces of the guanine dG and cytosine dC bases and, consequently, its denaturant behavior [11,38,39]. According to data reported in Figure 3, we can conclude that, although urea at these concentrations does not denature sDNA, it plays a minor role in its stabilization driven by the DES. The higher thermal energy required for the unstacking of guanine pairs in hydrated ChCl:U with respect to sDNA in buffer suggests a significant effect of DES on the double helix structure stability. Several simulation studies [15,40–42] report on the ability of choline ions to bind DNA around dG-dC base pairs in the major groove. Indeed, choline competes with those atoms that form dG-dC base pairs because of the attraction between its strongly polarized hydroxyl group and the negatively charged oxygen atoms of the bases. Although this behavior has been always connected to a destabilization effect, especially for dG-dC-rich duplex and single strand, little experimental data support this hypothesis. On the other hand, the melting temperatures (T_m) reported in [15] for ChCl/DNA solutions show that the T_m values increase at increasing the dG-dC base pair content and Pal et al. [10] have recently described the enhanced stability of the G-quadruplex in ChCl:U. Furthermore, the data in Figure 3c–f reveal that a greater concentration of ChCl:U in water does not produce a marked improvement in the transition temperature of sDNA. As a matter of fact, a threefold increase in ChCl:U in water coincides with an upturn of T_t for sDNA of only 2 K. This finding could be related to the specific characteristics of DES in solution and the prevalence of DES–DES over DES–sDNA interactions as the ChCl:U concentration increases. It is widely reported in the literature that the presence of water weakens the strong interactions among ChCl:U components and contributes to different solvation features of the individual DES components [43–45]. In this regard, we can consider the lowest concentration sample as a highly diluted solution of ChCl:U (i.e., 15 mol DES:1 mol H_2O), in which the DES individual components may exchange the ligands of their solvation shell by binding to DNA guanine moieties, i.e., by establishing hydrogen bonding, and thus exert their thermal stabilizing effect. This effect is offset by increasing the DES concentration

due to the re-establishment of interactions among each DES component to the detriment of the DES–sDNA H-bonds, thus reducing further structural modifications on sDNA. The thermal pathway of the dGI band for sDNA in the more concentrated solution of ChCl:U (Figure 3c) also shows a reversible increase in the Raman intensity between about 300 and 335 K. This suggests the occurrence of local structural changes in the geometry of the guanine bases relative to each other prior to the main structural transition of sDNA at 352 K. A temperature behavior similar to that described for the dGI band of sDNA is found also for the intensity of the signal dA + dG at ~1336 cm^{-1}. Figure S1a–c in the SI section shows the temperature-dependent trend exhibited by the intensity of this Raman band with the characteristic sharp increment in correspondence of the same transition temperatures T_t found for sDNA and sDNA in DES by the analysis of the dGI band (see also first derivative curves reported in Figure S1d–f). This outcome suggests that in the 250 nm-excited UVRR spectra of DNA both the two Raman signals identified as dGI and dA + dG are sensitive descriptors of the cooperative base-stacking interactions of the guanine bases during the thermal pathway of sDNA dissolved in different aqueous environments. Figure 4a–c display the temperature-dependence of the wavenumber position for the Raman signals dGI, dA + dG and dT for the sDNA duplex in Tris and hydrated ChCl:U, respectively. The observed downshift in the dGI band of sDNA upon the increment in temperature (Figure 4a) has been attributed to the formation of stronger H-bonds between the solvent and the guanine N7, occurring in the melted structure of DNA [18,19,24,26]. As mentioned above, DES induces a further red-shift of the position of the dGI band that persists over all the explored temperature ranges. We can ascribe this issue to the lessening of the H-bond attraction between the water molecules and the N7 site of guanine because of the competition with the greater interactions towards the DES [46]. This strong affinity helps the DES molecules to disrupt the well-coordinated hydration layer of water around the DNA structure and takes part in the solvation process. This outcome recalls the so-called "dehydration" phenomenon operated by some types of ionic liquids on the structure of the DNA duplex and predicted by simulation results [47,48]. We can argue that guanine bases experience stronger H-bonds with choline at the acceptor sites compared to water and that these interactions are also supposed to improve the stability of the B-form of DNA in the aqueous environment [15]. Interestingly, Figure 4a points out that the effect of a downshift on the dGI band is more evident for the lowest concentration of ChCl:U, consistent with the solvation picture suggested above. Similar to the dGI intensity profiles, we compared the behavior of sDNA in hydrated DES with that of its components in the same concentrations of the sDNA/ChCl:U 1:158 sample. As shown in Figure 4a, the dGI band's frequencies for ChCl and urea are blue-shifted compared to both sDNA in Tris and the sDNA/ChCl:U samples at both concentrations. For urea, the dGI frequencies confirm its role as a water molecules' competitor for establishing H-bonds with the guanine residues already reported. The different trends in sDNA/ChCl and the sDNA/ChCl:U 1:158 deserve further explanation. We can hypothesize that when ChCl is in solution with sDNA, it preferably acts as a hydrogen-bonding enhancer on the N7 sites, besides water. This result relates to [6], for example, who tested the improved solubility of biomolecules with the use of an individual DESs' components because of the contrasting DES–water and DES–solutes interactions. In the case of DES, the predominant effect of choline ion is that of breaking the pre-existing bonds (i.e., red-shift) and the establishment of preferential interactions between choline and guanine. This may indicate that, despite the similar stabilizing action towards temperature, the choline cation's dehydration of sDNA occurs only when it exists as a DES component or with a cooperative influence of urea. Moreover, it has been reported [15] that when choline ions locate around dG-dC base pairs, they preferably bind to dC(O2), dG(O6), and dC(N3). As the wavenumber of the dGI band can also be interpreted as an indicator of the hydrogen bonding at the C6 = O site [34], the notable red-shift could be additionally assigned to the competing activity of the choline ions to access the hydrogen bonding acceptor sites within the dG-dC base pairs once in ChCl:U. This effect seems to be confirmed also by the temperature behavior observed for the dA + dG signal in Figure 4b

that shifts to a lower frequency during thermal denaturation of sDNA. This red-shift can be ascribed to the sensitivity of the Raman band at ~1336 cm^{-1} to the local conformational changes involving both the dG and dA residues [22,27]. For sDNA/ChCl:U 1:158, the marked red-shift of this mode could be caused by the weakening of the H bonding at the acceptor sites (N1 and N6). Notably, choline is supposed to bind to the amino group in the dA-dT major grooves within sites dA(N6) and dA(N1) [15].

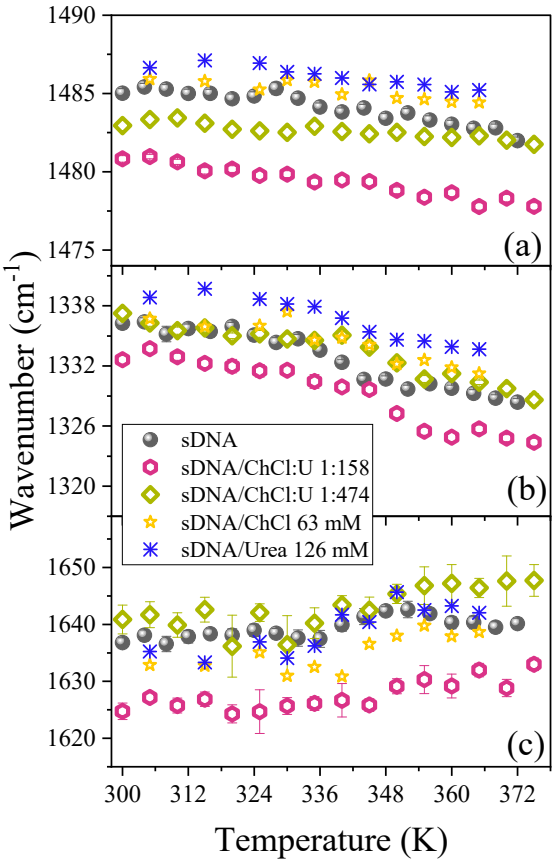

Figure 4. Temperature evolution of the central wavenumber position of the Raman bands (**a**) dGI, (**b**) dA + dG, and (**c**) dT for sDNA in the absence and presence of ChCl:U (1:158 and 1:474 ratio of molar concentrations) and sDNA in hydrated in ChCl (63 mM in Tris) and in hydrated urea (126 mM in Tris).

Figure 4c displays the temperature dependence wavenumber position of the dT band whose strength of oscillation accounts for any perturbations occurring at the C4 = O site of the thymine residue [22,33,34]. The upshift of this mode observed at ~335–345 K for sDNA can be correlated with a decrease in the hydrogen-bonding strength on the C=O site of thymine during the structural transition of sDNA occurring at the transition temperature [22,33]. The overall red-shift observed for the dT band for sDNA/ChCl:U 1:158 could be consistent with the establishment of strong interactions between the DES molecules and thymine C=O site at this specific concentration of ChCl:U.

Figure 5 displays the CD spectra collected at room temperature for sDNA dissolved in Tris buffer and in the ChCl:U/Tris solutions at the two concentration of DES in water.

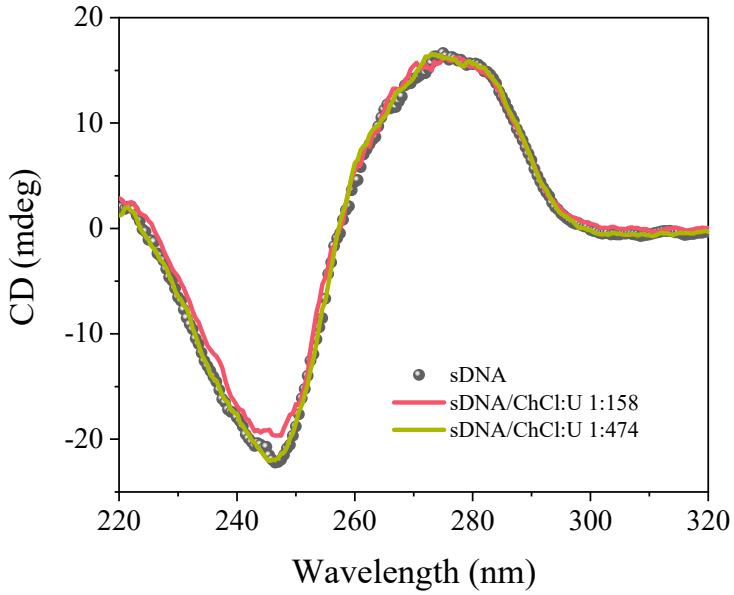

Figure 5. Comparison among the Circular Dichroism (CD) spectra collected at room temperature for sDNA and sDNA/ChCl:U (1:158 and 1:474).

The CD signal of sDNA exhibits the classical features of double-stranded B-form DNA, consisting of a positive band around 274 nm and a negative band at 245 nm with a crossover at the absorption maximum. The positive feature is due to base stacking, while the negative band is related to the polynucleotide helicity.

As a first remark, the comparison between the traces in Figure 5 shows that the CD spectra of sDNA with and without the DES have similar shapes, thus suggesting that the native B-conformation of DNA is preserved also after the addition of ChCl:U. This finding supports the predicted capability of a choline-based DES to preserve the native structure of DNA [49]. By looking at the curves in Figure 5, it appears that the presence of ChCl:U does not induce any significant change in the positive band at about 274 nm of sDNA. This is observed for both the two concentrations of DES in Tris considered in this work, namely, 63 and 189 mM. According to these data, the addition of DES to the solution of sDNA does not significantly affect the stacking interactions of base pairs in the structure of DNA at room temperature. This conclusion also confirms the UVRR results discussed above. Hence, the spectra in Figure 5 shows a slight increase in the negative molar ellipticity from −22 to −19 mdeg for the sDNA/ChCl:U 1:158 sample. Such behavior suggests a certain distortion in the helical structure of DNA in the hydrated DES. This could be consistent with the formation of stronger H-bonds between the guanine bases and DES choline, signified by the down shift of the wavenumber position for the dGI band. Interestingly, CD measurements seem to confirm the picture in which, at a concentration of DES above a certain critical value, the interactions among the ChCl:U components and/or the DES–water interactions tend to prevail against the formation of guanine–urea H-bonds.

5. Conclusions

The present study outlines the interplays between a hydrated ChCl:U DES and double-strand sDNA using a combined UVRR and CD approach. We investigated the guanine moieties' thermal pathways to define the stabilization exerted by the choline ions against sDNA's H-bond breaking and base unstacking. In this sense, both the sDNA samples in the DES show higher transition temperatures than in the buffer solution. According to the UVRR results, the increased interaction between ChCl:U and sDNA is due to the preferential binding between the choline ion and guanine, adenine, and thymine residues. In particular, the Raman band shifts reflect the changes in the hydrogen-bonding state on the bases' proton-acceptor sites. Urea seems to play a minor role in the solvation of double

strands, taking part as an enhancer of hydrogen bonding. Interesting information comes from the DESs' concentration dependence on the sDNA's thermal stability. Our preliminary results show that as the ChCl:U concentration increases, DES–DES interactions prevail on DES–sDNA ones, minimizing DES-induced structural stabilization effects. Overall, our study confirms the excellent physical–chemical properties of ChCl:U DES as a co-solvent for biomolecules, able to not only ensure sDNA solubility but also providing increased stability to temperature-induced conformational alterations.

Supplementary Materials: The following are available online at https://www.mdpi.com/article/10.3390/cryst11091057/s1, Figure S1. (**a**)–(**c**) Temperature dependence of the Raman intensity of dA + dG band for sDNA and sDNA/ChCl:U (1:158 and 1:474); panel (**b**) shows also the temperature profiles of dA + dG band obtained for sDNA in hydrated choline chloride (63 mM in Tris) and in hydrated urea (126 mM in Tris). (**d**)–(**f**) First derivative curves of the temperature profiles (**a**)–(**c**), respectively; the transition temperatures T_t obtained for sDNA without and with DES are marked in the corresponding panels.

Author Contributions: Conceptualization, M.T. and B.R.; data curation, M.T., J.V., I.M. and B.R.; funding acquisition, C.M.; investigation, M.T. and B.R.; resources, A.M.; software, A.G.; supervision, B.R.; validation, A.M. and B.R.; visualization, M.T.; writing—original draft, M.T. and B.R.; writing—review and editing, M.T., J.V., I.M., A.M. and B.R. All authors have read and agreed to the published version of the manuscript.

Funding: This research received no external funding.

Acknowledgments: We acknowledge CERIC-ERIC Consortium for the access to experimental facilities and financial support (proposal number 20202148). M.T. acknowledges the InCIMa4 project, funded by the European Regional Development Fund and Interreg V-A Italy Austria 2014–2020.

Conflicts of Interest: The authors declare no conflict of interest.

References

1. Martins, M.A.R.; Pinho, S.P.; Coutinho, J.A.P. Insights into the Nature of Eutectic and Deep Eutectic Mixtures. *J. Solut. Chem.* **2019**, *48*, 962–982. [CrossRef]
2. Zhang, Q.; De Oliveira Vigier, K.; Royer, S.; Jérôme, F. Deep Eutectic Solvents: Syntheses, Properties and Applications. *Chem. Soc. Rev.* **2012**, *41*, 7108–7146. [CrossRef]
3. Smith, E.L.; Abbott, A.P.; Ryder, K.S. Deep Eutectic Solvents (DESs) and Their Applications. *Chem. Rev.* **2014**, *114*, 11060–11082. [CrossRef]
4. Kist, J.A.; Zhao, H.; Mitchell-Koch, K.R.; Baker, G.A. The study and application of biomolecules in deep eutectic solvents. *J. Mater. Chem. B* **2021**, *9*, 536–566. [CrossRef]
5. Vilková, M.; Płotka-Wasylka, J.; Andruch, V. The role of water in deep eutectic solvent-base extraction. *J. Mol. Liq.* **2020**, *304*, 112747. [CrossRef]
6. Oliveira, G.; Wojeicchowski, J.P.; Oliveira Farias, F.; Igarashi-Mafra, L.; de Pelegrini Soares, R.; Mafra, M.R. Enhancement of biomolecules solubility in aqueous media using designer solvents as additives: An experimental and COSMO-based models' approach. *J. Mol. Liq.* **2020**, *318*, 114266. [CrossRef]
7. Cao, C.; Nian, B.; Li, Y.; Wu, S.; Liu, Y. Multiple Hydrogen-Bonding Interactions Enhance the Solubility of Starch in Natural Deep Eutectic Solvents: Molecule and Macroscopic Scale Insights. *J. Agric. Food Chem.* **2019**, *67*, 12366–12373. [CrossRef]
8. Pogozelski, W.K.; Tullius, T.D. Oxidative strand scission of nucleic acids: Routes initiated by hydrogen abstraction from the sugar moiety. *Chem. Rev.* **1998**, *98*, 1089–1108. [CrossRef]
9. Cadet, J.; Delatour, T.; Douki, T.; Gasparutto, D.; Pouget, J.P.; Ravanat, J.L.; Sauvaigo, S. Hydroxyl radicals and DNA base damage. *Mutat. Res. Fundam. Mol. Mech. Mutagen.* **1999**, *424*, 9–21. [CrossRef]
10. Pal, S.; Paul, S. Understanding the Role of Reline, a Natural DES, on Temperature-Induced Conformational Changes of C-Kit G-Quadruplex DNA: A Molecular Dynamics Study. *J. Phys. Chem. B* **2020**, *124*, 3123–3136. [CrossRef]
11. Nordstrom, L.J.; Clark, C.A.; Andersen, B.; Champlin, S.M.; Schwinefus, J.J. Effect of Ethylene Glycol, Urea, and N-Methylated Glycines on DNA Thermal Stability: The Role of DNA Base Pair Composition and Hydration. *Biochemistry* **2006**, *45*, 9604–9614. [CrossRef] [PubMed]
12. Mondal, D.; Mukesh, S.; Chandrakant, M.; Vishal, G.; Kamalesh, P. Improved solubility of DNA in recyclable and reusable bio-based deep eutectic solvents with long-term structural and chemical stability. *Chem. Commun.* **2013**, *49*, 9606–9608. [CrossRef] [PubMed]
13. de La Harpe, K.; Kohl, F.R.; Zhang, Y.; Kohler, B. Excited-State Dynamics of a DNA Duplex in a Deep Eutectic Solvent Probed by Femtosecond Time-Resolved IR Spectroscopy. *J. Phys. Chem. A* **2018**, *122*, 2437–2444. [CrossRef] [PubMed]

14. Mamajanov, I.; Engelhart, A.; Bean, H.; Hud, N. DNA and RNA in Anhydrous Media: Duplex, Triplex, and G-Quadruplex Secondary Structures in a Deep Eutectic Solvent. *Angew. Chem. Int. Ed.* **2010**, *49*, 6310–6314. [CrossRef] [PubMed]
15. Nakano, M.; Tateishi-Karimata, H.; Tanaka, S.; Sugimoto, N. Choline Ion Interactions with DNA Atoms Explain Unique Stabilization of A–T Base Pairs in DNA Duplexes: A Microscopic View. *J. Phys. Chem. B* **2014**, *118*, 379–389. [CrossRef]
16. Sequeira, R.A.; Bhatt, J.; Prasad, K. Recent Trends in Processing of Proteins and DNA in Alternative Solvents: A Sustainable Approach. *Sustain. Chem.* **2020**, *1*, 10. [CrossRef]
17. Abbott, A.P.; Capper, G.; Davies, D.L.; Rasheed, R.K.; Tambyrajah, V. Novel Solvent Properties of Choline Chloride/Urea Mixtures. *Chem. Commun.* **2003**, *1*, 70–71. [CrossRef]
18. Bottari, C.; Catalini, S.; Foggi, P.; Mancini, I.; Mele, A.; Perinelli, D.R.; Paciaroni, A.; Gessini, A.; Masciovecchio, C.; Rossi, B. Base-specific pre-melting and melting transitions of DNA in presence of ionic liquids probed by synchrotron-based UV resonance raman scattering. *J. Mol. Liq.* **2021**, *330*, 115433. [CrossRef]
19. Bottari, C.; Mancini, I.; Mele, A.; Gessini, A.; Masciovecchio, C.; Rossi, B. Conformational stability of DNA in hydrated ionic liquid by synchrotron-based UV resonance raman. In *UV and Higher Energy Photonics: From Materials to Applications 2019*; International Society for Optics and Photonics: Bellingham, WA, USA, 2019.
20. Rossi, B.; Bottari, C.; Catalini, S.; Gessini, A.; D'Amico, F.; Masciovecchio, C. Synchrotron based UV Resonant Raman scattering for material science. In *Molecular and Laser Spectroscopy*, 1st ed.; Gupta, V.P., Ozaki, Y., Eds.; Elsevier: Amsterdam, The Netherlands, 2020; Chapter 13; Volume 2, pp. 447–478.
21. Rossi, B.; Tortora, M.; Catalini, S.; Vigna, J.; Mancini, I.; Gessini, A.; Masciovecchio, C.; Mele, A. Insight into the thermal stability of DNA in hydrated ionic liquids from multi-wavelength UV resonance raman experiments. *Phys. Chem. Chem. Phys.* **2021**, *23*, 15980–15988. [CrossRef]
22. Fodor, S.P.A.; Rava, R.P.; Hays, T.R.; Spiro, T.G. Ultraviolet resonance Raman spectroscopy of the nucleotides with 266-, 240-, 218-, and 200-nm pulsed laser excitation. *J. Am. Chem. Soc.* **1985**, *107*, 1520–1529. [CrossRef]
23. Fodor, S.P.A.; Spiro, T.G. Ultraviolet resonance Raman spectroscopy of DNA with 200-266-nm laser excitation. *J. Am. Chem. Soc.* **1986**, *108*, 3198–3205. [CrossRef]
24. Bianchi, F.; Comez, L.; Biehl, R.; D'Amico, F.; Gessini, A.; Longo, A.M.; Masciovecchio, C.; Petrillo, C.; Radulescu, A.; Rossi, B.; et al. Structure of human telomere G-quadruplex in the presence of a model drug along the thermal unfolding pathway. *Nucleic Acids Res.* **2018**, *46*, 11927–11938. [CrossRef] [PubMed]
25. Wen, Z.Q.; Thomas, G.J., Jr. UV resonance raman spectroscopy of DNA and protein constituents of viruses: Assignments and cross sections for excitations at 257, 244, 238, and 229 nm. *Biopolymers* **1998**, *45*, 247–256. [CrossRef]
26. Duguid, J.G.; Bloomfield, V.A.; Benevides, J.M.; Thomas, G.J. DNA melting investigated by differential scanning calorimetry and Raman spectroscopy. *Biophys. J.* **1996**, *71*, 3350–3360. [CrossRef]
27. Duguid, J.G.; Bloomfield, V.A.; Benevides, J.M.; Thomas, G.J., Jr. Raman Spectroscopy of DNA-Metal Complexes. I. The Thermal Denaturation of DNA in the Presence of $Sr2^{+}$, Ba2, $Mg2^{+}$, $Ca2^{+}$, $Mn2^{+}$, $C02^{+}$, $Ni2^{+}$, and $Cd2^{+}$. *Biophys. J.* **1995**, *69*, 2623–2641. [CrossRef]
28. Toyama, A.; Takeuchi, H.; Harada, I. Ultraviolet resonance Raman spectra of adenine, uracil and thymine derivatives in several solvents. Correlation between band frequencies and hydrogen-bonding states of the nucleic acid bases. *J. Mol. Struct.* **1991**, *242*, 87–98. [CrossRef]
29. Turpin, P.Y.; Chinsky, L.; Laigle, A.; Jollès, B. DNA structure studies by resonance Raman spectroscopy. *J. Mol. Struct.* **1989**, *214*, 43–70. [CrossRef]
30. Erfurth, S.C.; Peticolas, W.I.S. Melting and premelting phenomenon in DNA by laser Raman scattering. *Biopolymers* **1975**, *14*, 247–264. [CrossRef]
31. Tsuboi, M.; Komatsu, M.; Hoshi, J.; Kawashima, E.; Sekine, T.; Ishido, Y.; Russell, M.P.; Benevides, J.M.; Thomas, G.J. Raman and Infrared Spectra of (2′S)-[2′-2H] Thymidine: Vibrational Coupling between Deoxyribosyl and Thymine Moieties and Structural Implications. *J. Am. Chem. Soc.* **1997**, *119*, 2025–2032. [CrossRef]
32. Jirasek, A.; Schulze, H.G.; Hughesman, C.; Creagh, A.L.; Haynes, C.A.; Blades, M.W.; Turner, R.F.B. Discrimination between UV radiation-induced and thermally induced spectral changes in AT-paired DNA oligomers using UV resonance raman spectroscopy. *J. Raman Spectrosc.* **2006**, *37*, 1368–1380. [CrossRef]
33. Mukerji, I.; Williams, A.P. UV resonance raman and circular dichroism studies of a DNA duplex containing an A(3)T(3) tract: Evidence for a premelting transition and three-centered H-bonds. *Biochemistry* **2002**, *41*, 69–77. [CrossRef]
34. Toyama, A.; Hanada, N.; Ono, J.; Yoshimitsu, E.; Takeuchi, H. Assignments of guanosine UV resonance raman bands on the basis of ^{13}C, ^{15}N and ^{18}O substitution effects. *J. Raman Spectrosc.* **1999**, *30*, 623–630. [CrossRef]
35. Movileanu, L.; Benevides, J.M.; Thomas, G.J., Jr. Temperature Dependence of the Raman Spectrum of DNA. Part I—Raman Signatures of Premelting and Melting Transitions of Poly(dA–dT)·Poly(dA–dT). *J. Raman Spectrosc.* **1999**, *30*, 637–649. [CrossRef]
36. Gállego, I.; Grover, M.A.; Hud, N.V. Folding and Imaging of DNA Nanostructures in Anhydrous and Hydrated Deep-Eutectic Solvents. *Angew. Chem. Int. Ed.* **2015**, *54*, 6765–6769. [CrossRef]
37. Oprzeska-Zingrebe, E.A.; Smiatek, J. Preferential Binding of Urea to Single-Stranded DNA Structures: A Molecular Dynamics Study. *Biophys. J.* **2018**, *114*, 1551–1562. [CrossRef]

38. Hong, J.; Capp, M.W.; Anderson, C.F.; Saecker, R.M.; Felitsky, D.J.; Anderson, M.W.; Record, M.T., Jr. Preferential interactions of glycine betaine and of urea with DNA: Implications for DNA hydration and for effects of these solutes on DNA stability. *Biochemistry* **2004**, *43*, 14744–14758. [CrossRef]
39. Herskovits, T.T. Nonaqueous Solutions of DNA; Denaturation by Urea and Its Methyl Derivatives. *Biochemistry* **1963**, *2*, 335–340. [CrossRef] [PubMed]
40. Tateishi-Karimata, H.; Sugimoto, N. Structure, stability and behaviour of nucleic acids in ionic liquids. *Nucleic Acids Res.* **2014**, *42*, 8831–8844. [CrossRef]
41. Tateishi-Karimata, H.; Sugimoto, N. A–T Base Pairs are More Stable Than G–C Base Pairs in a Hydrated Ionic Liquid. *Angew. Chem. Int. Ed.* **2012**, *51*, 1416–1419. [CrossRef]
42. Portella, G.; Germann, M.W.; Hud, N.V.; Orozco, M. MD and NMR Analyses of Choline and TMA Binding to Duplex DNA: On the Origins of Aberrant Sequence-Dependent Stability by Alkyl Cations in Aqueous and Water-Free Solvents. *J. Am. Chem. Soc.* **2014**, *136*, 3075–3086. [CrossRef]
43. Shobhna, K.P.; Kaur, S.; Kashyap, H.K. Influence of Hydration on the Structure of Reline Deep Eutectic Solvent: A Molecular Dynamics Study. *ACS Omega* **2018**, *3*, 15246–15255.
44. Di Pietro, M.E.; Hammond, O.; van den Bruinhorst, A.; Mannu, A.; Padua, A.; Mele, A.; Costa Gomes, M. Connecting chloride solvation with hydration in deep eutectic systems. *Phys. Chem. Chem. Phys* **2021**, *21*, 107–111. [CrossRef] [PubMed]
45. Shah, D.; Mjalli, F.S. Effect of water on the thermo-physical properties of Reline: An experimental and molecular simulation based approach. *Phys. Chem. Chem. Phys* **2014**, *16*, 23900–23907. [CrossRef] [PubMed]
46. Duguid, J.G.; Bloomfield, V.A.; Benevides, J.M.; Thomas, G.J. Raman Spectroscopy of DNA-Metal Complexes. 1. Interactions and Conformational Effects of the Divalent Cations: Mg, Ca, Sr, Ba, Mn, Co, Ni, Cu, Pd, and Cd. *Biophys. J.* **1993**, *65*, 1916–1928. [PubMed]
47. Chandran, A.; Ghoshdastidar, D.; Senapati, S. Groove Binding Mechanism of Ionic Liquids: A Key Factor in Long-Term Stability of DNA in Hydrated Ionic Liquids. *J. Am. Chem. Soc.* **2012**, *134*, 20330–20339. [CrossRef]
48. Jumbri, K.; Abdul Rahman, M.B.; Abdulmalek, E.; Ahmada, H.; Micaelo, N.M. An insight into structure and stability of DNA in ionic liquids from molecular dynamics simulation and experimental studies. *Phys. Chem. Chem. Phys.* **2014**, *16*, 14036–14046. [CrossRef]
49. Zhao, H. DNA stability in ionic liquids and deep eutectic solvents. *J. Chem. Technol. Biotechnol.* **2015**, *90*, 19–25. [CrossRef] [PubMed]